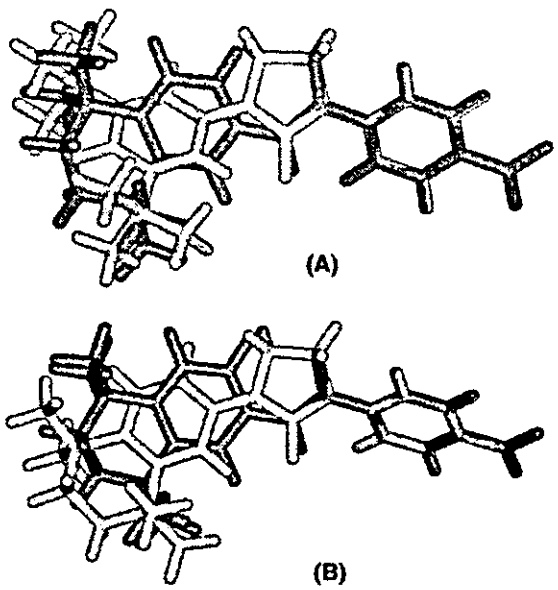

Figure 4. (A) Superimposition of energy-minimized conformations of YR105 (green) and Am80 (red). (B) Superimposition of energy-minimized conformations of YR107 (green) and Am80 (red).

(5f), YR107 (5g) decreased the activity by two orders of magnitude, compared with YR105.

Figure 4 shows superimposition of the energy-minimized structures of YR105 (5e) and YR107 (5g) on the energy-minimized structure Am80. YR105 is better overlapped with Am80 than YR107.

A docking model of YR105 (5e) bound to RARγ (1EXA) was constructed by molecular dynamics (MD) simulation at high temperature (1000 K) and molecular mechanics (MM) energy minimization. AMBER* was used as force field. Calculations were performed by *MacroModel* (ver. 6.5 and 8.0).[9] YR105 was well fitted to the cavity of the ligand binding domain (LBD) of RARγ, as shown in Figure 5. The bulky alkylated phenyl moiety fits well to the hydrophobic region of the LBD (Trp-227, Phe-230, Leu-268, Phe-304, Leu-307, Ala-397, Ile-412, Leu-416). The carboxylate group of the ligand interacted with Arg-278, Ser-289 by hydrogen bonds.

In conclusion, we have discovered a new class of cyclic urea compounds that exhibit retinoidal activity.

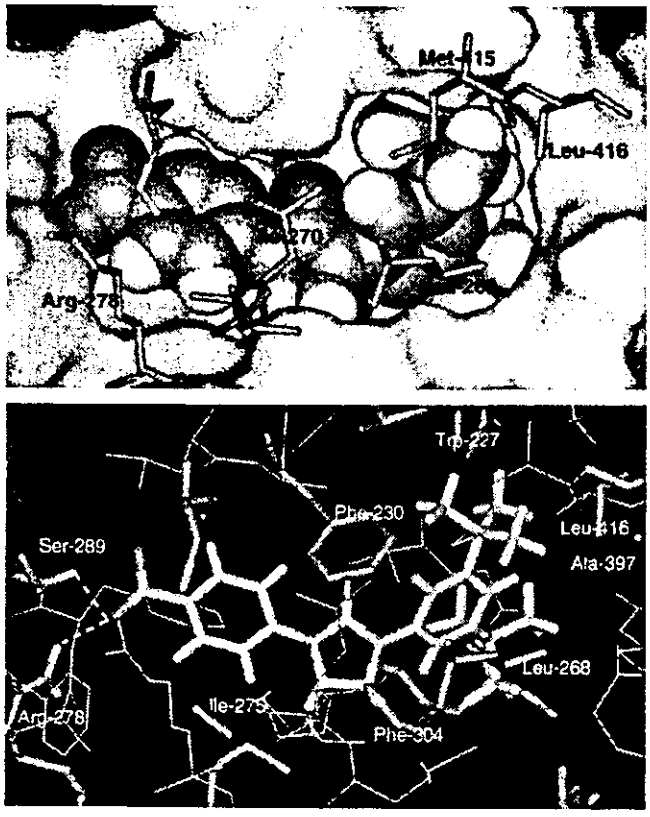

Figure 5. Stable docking model of 5e (YR105) in the RARγ simulated from the crystal structure of RAR-BMS270394 complex (1EXA).

Acknowledgements

This work was supported in part by a grant (MF-16) from the Organization for Pharmaceutical Safety and Research and by the Budget for Nuclear Research of the Ministry of Education, Culture, Sports, Science and Technology, based on the screening and counseling by the Atomic Energy Commission.

References and notes

1. *The Retinoids*, 2nd ed.; Sporn, M. B., Roberts, A. B., Goodman, D. S., Eds.; Raven: New York, 1994.
2. Hill, D. L.; Grubbs, C. *J. Annu. Rev. Nutr.* **1992**, *12*, 161–181.
3. Chomienne, C.; Fenaux, P.; Degos, L. *FASEB J.* **1996**, *10*, 1025–1030.
4. Kagechika, H.; Kawachi, E.; Fukusawa, H.; Saito, G.; Iwanami, N.; Umemiya, H.; Hashimoto, Y.; Shudo, K. *Biochem. Biophys. Res. Commun.* **1997**, *231*, 243–248.
5. Leid, M.; Kastner, P. *Trends Biochem. Sci.* **1992**, *17*, 427, and references cited therein.
6. (a) Hashimoto, Y.; Kagechika, H.; Shudo, K. *Biochem. Biophys. Res. Commun.* **1990**, *166*, 1300–1307; (b) Matsushima, Y.; Kawachi, E.; Tanaka, H.; Kagechika, H.; Hashimoto, Y.; Shudo, K. *Biochem. Biophys. Res. Commun.* **1992**, *189*, 1136–1142; (c) Hashimoto, Y.; Kagechika, H.; Kawachi, E.; Fukasawa, H.; Saito, G.; Shudo, K. *Biol. Pharm. Bull.* **1996**, *19*, 1322–1328; (d) Umemiya, H.; Fukusawa, H.; Ebisawa, M.; Eyrolles, L.; Kawachi, E.; Eisenmann, G.; Gronemeyer, H.; Hashimoto, Y.; Shudo, K.; Kagechika, H. *J. Med. Chem.* **1997**, *40*, 4222–4234; (e) Koch, S. S. C.; Dardashti, L. I.; Rosemary, M. C.; Croston, C. E.; Boehm, M. F.; Heyman, R. A.; Nadzan, A. M. *J. Med. Chem.* **1999**, *42*, 742–750; (f) Nagy, L.; Thomazy, V. A.; Shipley, G. L.; Fesus, L.; Lamph, W.; Heyman, R. A.; Chandraratna, R. A. S.; Davies, P. J. A. *Mol. Cell. Biol.* **1995**, *15*, 3540–3551; (g) Endo, Y.; Iijima, T.; Yaguchi, K.; Kawachi, E.; Inoue, N.; Kagechika, H.; Kubo, A.; Itai, A. *Bioorg. Med. Chem. Lett.* **2001**, *11*, 1307–1311; (h) Kobayashi, N.; Kaku, Y.; Higurashi, K.; Yamauchi, T.; Ishibashi, A.; Okamoto, Y. *Bioorg. Med. Chem. Lett.* **2002**, *12*,

1747–1750; (i) Beard, R. L.; Duong, T. T.; Klein, E. S.; Standevan, A. M.; Chandraratna, R. A. S. *Bioorg. Med. Chem. Lett.* **2002**, *12*, 3145–3148.
7. Kagechika, H. *Yakugaku Zasshi* **1994**, *114*, 847–862.
8. Kagechika, H.; Himi, T.; Kawachi, E.; Shudo, K. *J. Med. Chem.* **1989**, *32*, 2292–2296.
9. (a) Kittaka, A.; Suhara, Y.; Takayanagi, H.; Fujishima, T.; Kurihara, M.; Takayama, H. *Org. Lett.* **2000**, *2*, 2619–2622; (b) Konno, K.; Fujishima, T.; Maki, S.; Liu, Z.; Miura, D.; Chokki, M.; Ishizuka, S.; Yamaguchi, K.; Kan, Y.; Kurihara, M.; Miyata, N.; Smith, C.; DeLuca, H. F.; Takayama, H. *J. Med. Chem.* **2000**, *43*, 4247–4265; (c) Fujishima, T.; Konno, K.; Nakagawa, K.; Tanaka, M.; Okano, T.; Kurihara, M.; Miyata, N.; Takayama, H. *Chem. Biol.* **2001**, *8*, 1011–1024 (2001); (d) Suhara, S.; Nihei, K.; Kurihara, M.; Kittaka, A.; Fujishima, T.; Konno, K.; Miyata, N.; Takayama, H. *J. Org. Chem.* **2001**, *66*, 8760–8771; (e) Uhara, Y.; Kittaka, A.; Ono, K.; Kurihara, M.; Fujishima, T.; Yoshida, A.; Takayama, H. *Bioorg. Med. Chem. Lett.* **2002**, *12*, 3533–3536; (f) Kittaka, A.; Kurihara, M.; Peleg, S.; Suhara, Y.; Takayama, H. *Chem. Pharm. Bull.* **2003**, *51*, 57–358.

Polycyclic Aromatic Compounds, 24: 487–500, 2004

ISSN: 1040-6638 print / 1563-5333 online
DOI: 10.1080/10406630490471500

Taylor & Francis
Taylor & Francis Group

ASSOCIATIONS BETWEEN CHEMICAL PROPERTIES AND OXIDATIVE DAMAGE DUE TO NITROPHENANTHRENES AND THEIR RELATED COMPOUNDS IN PRIMARY RAT HEPATOCYTES

Nobuyuki Sera
Fukuoka Institute of Health and Environmental Sciences, Dazaifu, Fukuoka, Japan
Hiroshi Tokiwa
Laboratory of Environmental Health Science, Kyushu Women's University, Yahatanishi-ku, Kitakyushu, Japan
Hideo Utsumi
Laboratory of Bio-Fuction Analysis, Graduate School of Pharmaceutical Sciences, Kyushu University, Higashi-ku, Fukuoka, Japan
Shigeki Sasaki
Bioorganic and Synthetic Chemistry, Graduate School of Pharmaceutical Sciences, Kyushu University, Higashi-ku, Fukuoka, Japan
Kiyoshi Fukuhara
Naoki Miyata
National Institute of Health Sciences, Setagaya-ku, Tokyo, Japan

Nitrated derivatives of phenanthrene, azaphenanthrene, and their N-oxides were synthesized, and their chemical properties, LUMO energy, the first and second reduction potentials, and dihedral angle of nitro groups were investigated. On orientation of 22 nitrophenanthrenes (NPhs), and 19 nitroazaphenanthrenes (NAPhs) containing their N-oxides (NPhOs), NPhs and NAPhs substituted at positions 2, 3, 6, and 7 were almost coplanar to the

Received 1 September 2003; accepted 1 February 2004.
Address correspondence to Nobuyuki Sera, Fukuoka Institute of Health and Environmental Sciences, 39 Mukaizano Dazaifu, Fukuoka 818-0135, Japan. E-mail: sera@fihes.pref.fukuoka.jp

aromatic ring, while those at positions 1, 5, 8, 9, and 10 were almost perpendicular. On the other hand, primary rat hepatocytes prepared from SD rats efficiently induced 8-oxodeoxyguanine (8-oxo-Gua) of 4-nitroquinoline N-oxide (4-NQO), a mutagen and carcinogen. 8-oxo-Gua formed due to oxidative damage was dose dependent at levels from 1.0 to 5.0 nM of 4-NQO. 8-oxo-Gua formation of NPhs and NAPhs in primary rat hepatocytes was determined, and the results significantly correlated with the first reduction potentials (r = 0.906) and LUMO energy (r = 0.874) of these derivatives. It was concluded that the nitro group of Phs and APhs were metabolized by the NADPH-cytochrome p450 enzyme in primary rat hepatocytes, and a radical anion of NPhs was induced. Finally, the hydroxyl radicals induced promoted hydroxylation at the 8 position of the guanine residue. It was found that these metabolic pathways were closely associated with the first reduction potentials, and the LUMO energy of NPhs and NAPhs, as well as 8-oxo-Gua formation were related to these chemical properties.

Keywords nitroazaphenanthrenes, nitrophenanthrenes, 8-oxodeoxyguanosine

Many investigators have discussed the association between the mutagenicity of nitrated polycyclic aromatic hydrocarbons (nPAHs) and their chemical structure (1–9). Nitrophenanthrene derivatives are ubiquitous mutagens in the environment, and distribute widely in diesel exhaust particulates (10). We have already reported that there was a relationship between *Salmonella* mutagenicity and orientation of nitrophenanthrenes (9) and nitroazaphenanthrenes (11). For *Salmonella* mutagenicity of nitrophenanthrenes (NPhs), nitro substituents that were almost coplanar in aromatic rings enhanced mutagenicity while those which were perpendicular in the rings reduced this activity (9–11). It was revealed that the mutagenic activity of NPhs was closely associated with reduction potentials and the dihedral angles of the nitro substituent for intercalation of chemicals into DNA (9, 11).

On the other hand, 8-hydroxyguanosine has been used as a biomarker of oxidative DNA damage in human lung tissue (12, 13), human leukocytes (14), and in the urinary tract (15). Furthermore, it was found that environmental substances such as diesel particles formed 8-hydroxyguanine in an in vivo test in mice, and that they were involved

in the generation of oxygen and hydroxyl radicals through phagocytosis of particles in macrophages (16).

In this study, it was demonstrated that there was a correlation between 8-oxodeoxyguanosine (8-oxo-Gua) formed in primary rat hepatocytes and the chemical properties of NPhs and their related compounds. It was found that the first reduction potentials and LUMO energy of nPAHs may be involved with 8-oxo-Gua formation through radical reactions in metabolic pathways.

MATERIALS AND METHODS

Chemicals

Nitrophenanthrenes (NPhs) used were 1-, 3-, and 9-NPhs; 1,5-, 1,6-, 1,10-, 2,6-, 2,9-, 2,10-, 3,5-, 3,6-, 3,10-, 4,9-, and 4,10-diNPhs; and 1,5,9-, 1,5,10-, and 3,6,9-triNPhs as reported previously (9). Nitroazaphenanthrenes (NAPhs) used were 8-nitro-1-azaphenanthrene (8-N-1-APh), 6- and 8-N-4-APhs, 4-, 5-, 6-, and 7-N-9-APhs, 5-, 6-, and 8-N-1-APh N-oxide (5-, 6-, and 8-N-1-APhO), 5-, 6-, and 8-N-4-APhOs, 1-, 2-, 3- and 5-N-9-APhOs, and 1,5- and 1,8-dinitro-4-APhOs (1,5- and 1,8-diN-4-APhOs) as reported previously (11, 17). 4-Nitroquinolin-N-oxide (4-NQO) was obtained from Sigma Chemical Company.

Electrochemical Reduction by Cyclic Voltammetry and Electronic Descriptors

The electronic descriptor and LUMO energy levels of chemicals were calculated by MOPAC 2002 (AM1), which is based on the MOPAC of the Toray System Center, using the AM1 method. The initial geometries were constructed from standard bond lengths and angles. The geometries were then completely optimized using algorithms in the MOPAC program. Electrochemical reduction by cyclic voltammetry was measured by the method described in a previous report (9, 11).

Preparation of Primary Rat Hepatocytes

Primary rat hepatocytes were isolated from male specific pathogen-free Sprague-Dawley rats, weighing 200 to 250 g (8 to 10 weeks of age), and plated on a collagen substratum of 12 well plates with Dulbecco's Modified Eagle Media (Ginco Co. Ltd.) supplemented with fetal calf serum (5%), insulin (6.25 μg/mL), penicillin (50 μ/mL), streptomycin (50 μg/mL), and dexamethasone (1M) at a density of 3×10^3 viable

cells/dish. The cells were preincubated in the 5% CO_2 at 37°C for 20 h, exposed to chemicals for 24 h, and then cultured for a further 20 h in fresh medium. Cell viability was assessed by Trypan blue. The concentration of dimethylsulfoxide (DMSO) or distilled water was below 0.5% to avoid any cytotoxic influence. DNA was isolated from cells lysed with 2% sodium dodecyl sulfate at 37°C for 30 min. Portions of DNA materials were dissolved in a 10 mM sodium acetate buffer (pH 4.8) digested with 20 mg nuclease P1 at 37°C for 30 min, and then treated with 1.3 units of *Escherichia coli* alkaline phosphomonoesterase in 0.1M Tris-HCl buffer (pH 7.5) for 1 h.

Determination of 8-Oxoguanine (8-oxo-Gua)

Determination of 8-oxo-Gua was performed using the method reported previously (11, 13). After rat hepatocytes were stored at −80°C for 2 h, the materials were fused for 30 min in a CO_2 incubator and homogenized in a lysis solution with a Pozter-type homogenizer. The DNA was isolated from rat hepatocytes using a DNA extractor WB kit according to the method reported by Inoue et al. (12). All procedures were performed in a stream of nitrogen to prevent any artifacts during the DNA extraction. An authentic 8-oxo-Gua sample added to the cells consistently yielded in the range of 92% to 94%. The extracted DNA was dissolved in 100 μL of 1 mM EDTA and digested with 4 μL of nuclease P1 (5 mg/mL) and 2 L of acid phosphatase (47 mg/mL) suspension in 1.8 M $(NH_4)_2SO_4$ in the presence of 20 mM sodium acetate buffer at pH 4.5. After incubation at 37°C, the mixture was treated with 10 μL of ion exchange resin, Muromac (Muromachi Kagaku Kogyo, Tokyo, suspension, 50 mg/mL), and centrifuged at 15,000 × g for 5 min. The supernant was transferred to a filter tube (Millipore, Bedford, Massachusetts, USA; Samprep C; 0.2 μm) and centrifuged at 5,000 × g for 5 min. Then, the filtrate was injected into a high-pressure liquid chromatography column (HPLC). The 8-oxo-Gua concentration was determined using the HPLC-electrochemical detector (ECD) method, and the level was measured as the mean value repeated in triplicate two times.

RESULTS

Reduction Potential, LUMO Energy Levels, and Dihedral Angles of NPhs and NAPhs

Figure 1 illustrates the chemical structures of phenanthrene (Ph), 1-, 4-, 9-APhs, and 1-, 4-, and 9-APhOs. In this study, 22 NPhs and

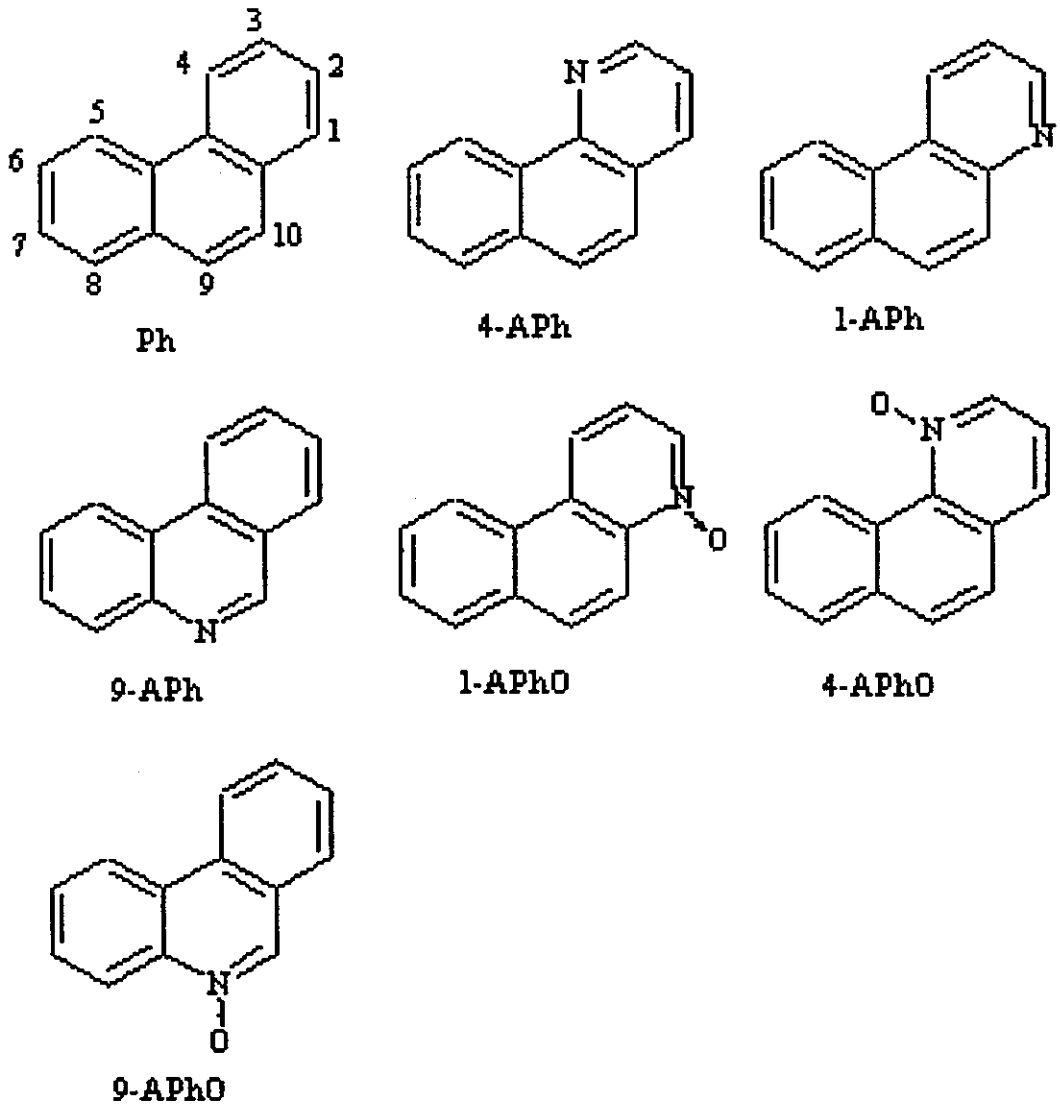

FIGURE 1. Chemical structures of phenanthrenes and their related compounds: APh, azaphenanthrene; APhO, azaphenanthrene N-oxide.

19 NAPhs, including their N-oxide derivatives, were synthesized; 1-, 3-, and 9-NPhs; 1,5-, 1,6-, 1,10-, 2,6-, 2,9-, 2,10-, 3,5-, 3,6-, 3,10-, 4,9-, and 4,10-diNPhs; 1,5,9-, 1,5,10-, 1,6,9-, 1,7,9-, 2,5,10-, 2,6,9-, 3,5,10-, and 3,6,9-triNPhs; 8-N-1-ANPh, 6- and 8-N-4-APhs, 4-, 5-, 6-, and 7-N-9-APhs; 5-, 6-, and 8-N-1-APhOs, 5-, 6-, and 8-N-4-APhOs, 1-, 2-, 3-, and 5-N-9-APhOs; 1,5- and 1,8-diN-4-APhOs. Tables 1 and 2 indicate the results for reduction potentials, LUMO energy levels, and orientation of NPhs and NAPhs. As shown in Table 1, NPhs substituted at the 1 and 8, 5 and 4, 9 and 10 positions in the phenanthrene rings were perpendicular or almost perpendicular due to the steric effect of the bay region aromatic proton, while those at the 2 and 7, 3 and 6 positions were almost

TABLE 1. LUMO Energy Levels and Dihedral Angles of Nitrophenanthrenes

Compound	Epc	LUMO	Dihedral angles (deg)
1-NPh	−1,477	−1.345	16.9
3-NPh	−1,453	−1.367	0.3
9-NPh	−1,450		11.1
1,5-diNPh	−1,373	−1.644	125
1,6-diNPh	−1,357	−1.937	19.1
1,10-diNPh	−1,336	−1.767	127.5
2,6-diNPh	−1,365	−1.836	2.8
2,9-diNPh	−1,311	−1.908	17.9
2,10-diNPh	−1,368	−1.901	15.7
3,5-diNPh	−1,363	−1.735	87.3
3,6-diNPh	−1,341	−1.955	0.5
3,10-diNPh	−1,242	−2.006	18.8
4,9-diNPh	−1,277	−1.880	112.7
4,10-diNPh	−1,297	−1.850	110.2
1,5,9-triNPh	−1,063	−2.345	151.6
1,5,10-triNPh	−1,150	−2.228	198.1
1,6,9-triNPh	−1,058	−2.528	51.6
1,7,9-triNPh	−1,058	−2.422	57.8
2,5,10-triNPh	−1,050	−2.186	174.3
2,6,9-triNPh	−1,116	−2.432	35.7
3,5,10-triNPh	−1,139	−2.394	122.1
3,6,9-triNPh	−1,042	−2.643	21.2

coplanar to the phenanthrene rings, showing dihedral angles from 0.3 to 2.8. Similarly, the chemical properties of NAPhs were also calculated, as shown in Table 2. NAPhs substituted at the 2 and 7, and 3 and 6 were almost coplanar, showing dihedral angles from 0.0 to 0.7 while those at the 1, 4, 5, and 8 were perpendicular or almost perpendicular to the aromatic rings. In addition, the calculated LUMO energy levels were in good correlation with the observed reduction potentials among NPhs and NAPhs; in particular, the LUMO energy levels were correlated with the first reduction potentials more than the second reduction potentials (Table 2).

As this study was to investigate whether or not these chemical properties were associated with 8-oxo-Gua formation in primary rat hepatocytes. Primary rat hepatocytes were prepared from male SD rats as described in the Materials and Methods section. The ability to form 8-oxo-Gua in the primary rat hepatocytes was investigated using 4-NQO, a potent carcinogen. The results were obtained with dose dependency for

TABLE 2. LUMO Energy Levels, Reduction Potentials, and Dihedral Angles of Nitroazaphenanthrenes

Chemical	Epc (mV)		LUMO	Dihedral angle
	Epc1	Epc2		
8-N-1-Aph	−1,042	−1,631	−1,429	31.5
6-N-4-Aph	−1,036	−1,675	−1,400	0.1
8-N-4-Aph	−1,058	1,555	−1,372	32.2
4-N-9-Aph	−1,120	−1,662	−1,326	62.6
5-N-9-Aph	−1,085	−1,615	−1,219	61.7
6-N-9-Aph	−1,027	−1,645	−1,508	0.2
7-N-9-Aph	−1,004	−1,664	−1,436	0
5-N-1-APhO	−1,049	−1,625	−1,505	61
6-N-1-APhO	−972	−1,572	−1,663	0.1
8-N-1-APhO	−988	−1,641	−1,623	33.3
5-N-4-APhO	−1,214	−1,619	−1,427	32.2[a]
6-N-4-APhO	−1,059	−1,723	−1,583	0.7
8-N-4-APhO	−1,047	−1,678	−1,545	31.7
1-N-9-APhO	−853	−1,484	−1,674	26.5
2-N-9-APhO	−964	−1,628	−1,696	0.1
3-N-9-APhO	−893	−1,463	−1,733	0.1
5-N-9-APhO	−1,029	−1,568	−1,494	60.3
1,5-diN-4-APho	−623	−1,263	−2,074	30.1[b]
1,8-diN-4-APho	−916	−1,032	−2,214	58.2*

*8-NO2, 33.5; 1-NO2, 24.7.

[a,b]LUMO energy and dihedral angle were obtained by AM1 calculations based on the structure that was optimized by PM3.

8-oxo-Gua formation at dose levels from 1 to 5 nM of 4-NQO (Figure 2), suggesting metabolic activation of cytochrome p450 in rat hepatocytes.

Figure 3 shows the correlation between the first reduction potentials of NPhs (a) and LUMO energy (b), and levels of 8-oxo-Gua formed in rat hepatocytes. The first reduction potentials of NPhs, but not the second reduction potentials, represented a significant correlation with 8-oxo-Gua levels ($r = 0.906$) (Figure 3a). In addition, the correlation between LUMO energy and 8-oxo-Gua levels was analyzed (Figure 3b). It was found that 8-oxo-Gua was strongly formed at lower LUMO energy levels from −1.345 to −2.643, and both agents were significantly correlated at a correlation factor of 0.874.

The first reduction potentials and LUMO energy levels of NAPhs were also determined, and the results are illustrated in Figure 4. Similarly, the first reduction potentials were involved with the metabolic reduction of the nitro group of PAHs and the involvement was more pronounced than

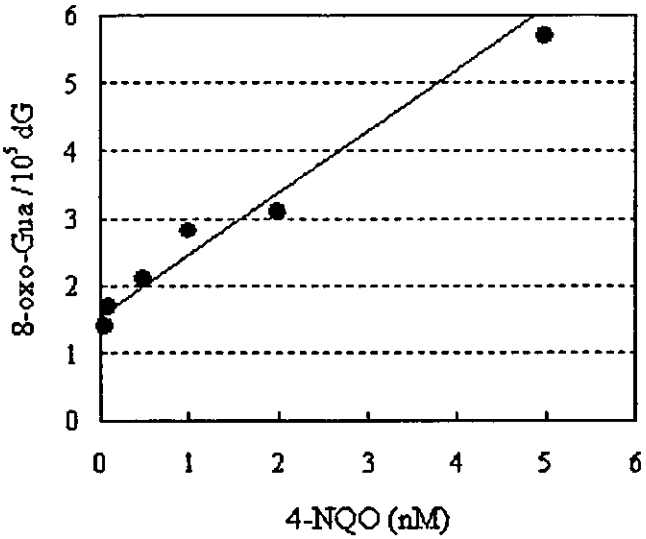

FIGURE 2. 8-oxo-Gua formation by 4-NQO in primary rat hepatocytes.

the second reduction potentials (data not shown). The first reduction potentials of mononitro-APhs were lower than those of dinitro-APhs (Table 2).

The 8-oxo-Gua formation of NPhs was significantly correlated with the first reduction potentials ($r = 0.924$) and also with LUMO energy levels, but was not significant ($r = 0.428$). The 8-oxo-Gua formation increased at the higher levels of the first reduction potentials, but was at lower levels of LUMO energy (Figure 4a, b).

Possible Mechanism of Oxygen Damage Due to NPhs and NAPhs

Modification of guanine residue on DNA due to oxygen damage was analyzed, and its chemical pathway is illustrated in Figure 5. Nitro groups of NPhs and NAPhs were metabolically reduced by the NADPH-cytochrome p450 enzyme in primary rat hepatocytes, and radical anions were induced at the 8-position of the guanine residue. Subsequently, reactive oxygen species as superoxides were generated, and hydroxyl radicals were generated in the presence of heme iron. Consequently, it was considered that 8-oxo-Gua was formed by the reactive hydroxyl radical at position 8 of the guanine residue.

DISCUSSION

We previously reported that the mutagenic potency of NPhs and NAPhs for *Salmonella* strains was closely correlated with the orientation

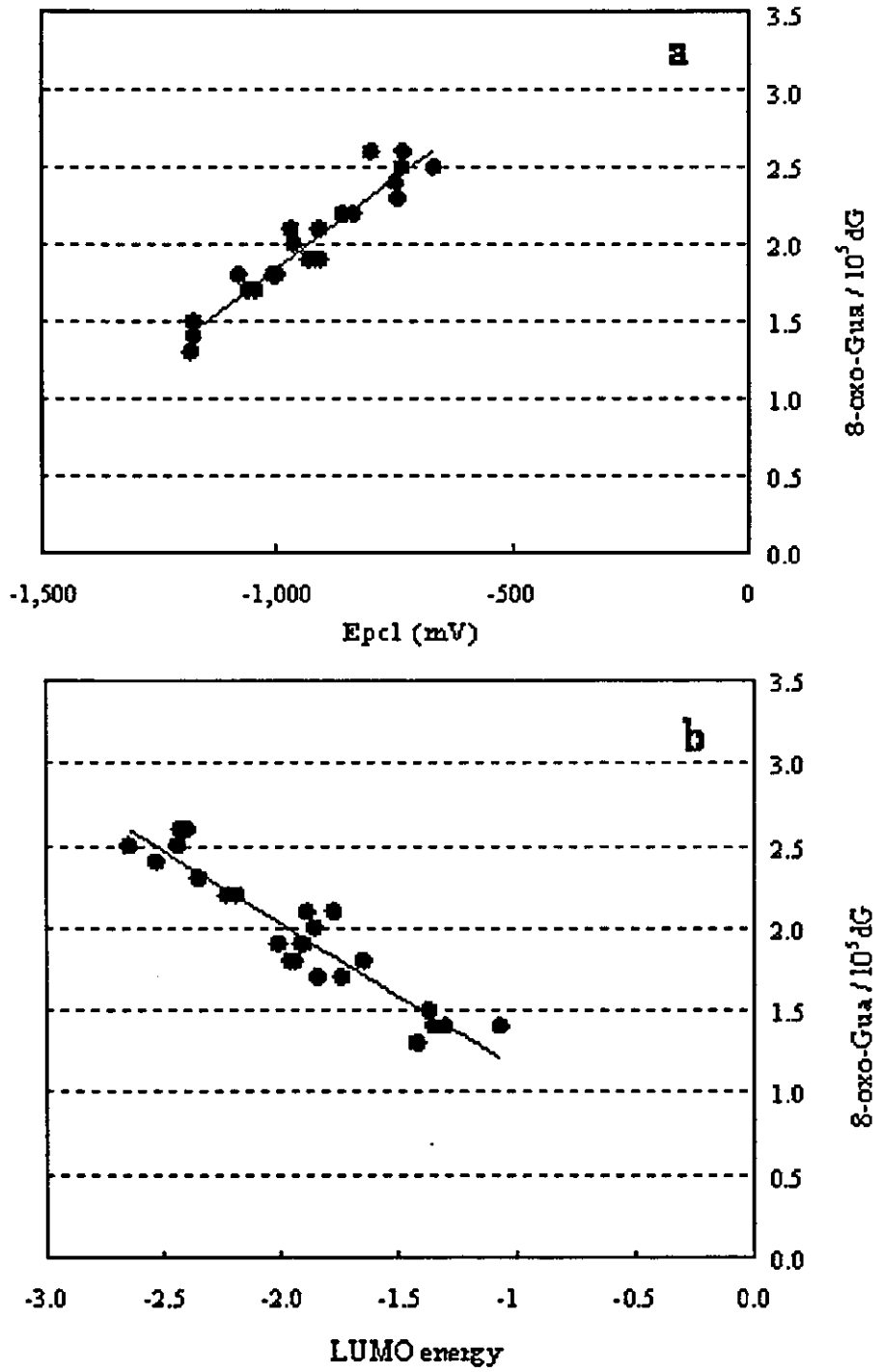

FIGURE 3. Correlation between 8-oxo-Gua formation, and the first reduction potentials (a), and LUMO energy (b) of NPhs. (a) $r = 0.906$; (b) $r = 0.874$.

of nitro substituents of aromatic rings and LUMO energy levels (9, 11). In fact, some derivatives substituted at positions 4 and 5 in the phenanthrene rings were perpendicular or almost perpendicular, and they were weak mutagens or nonmutagens. In contrast, those substituted on

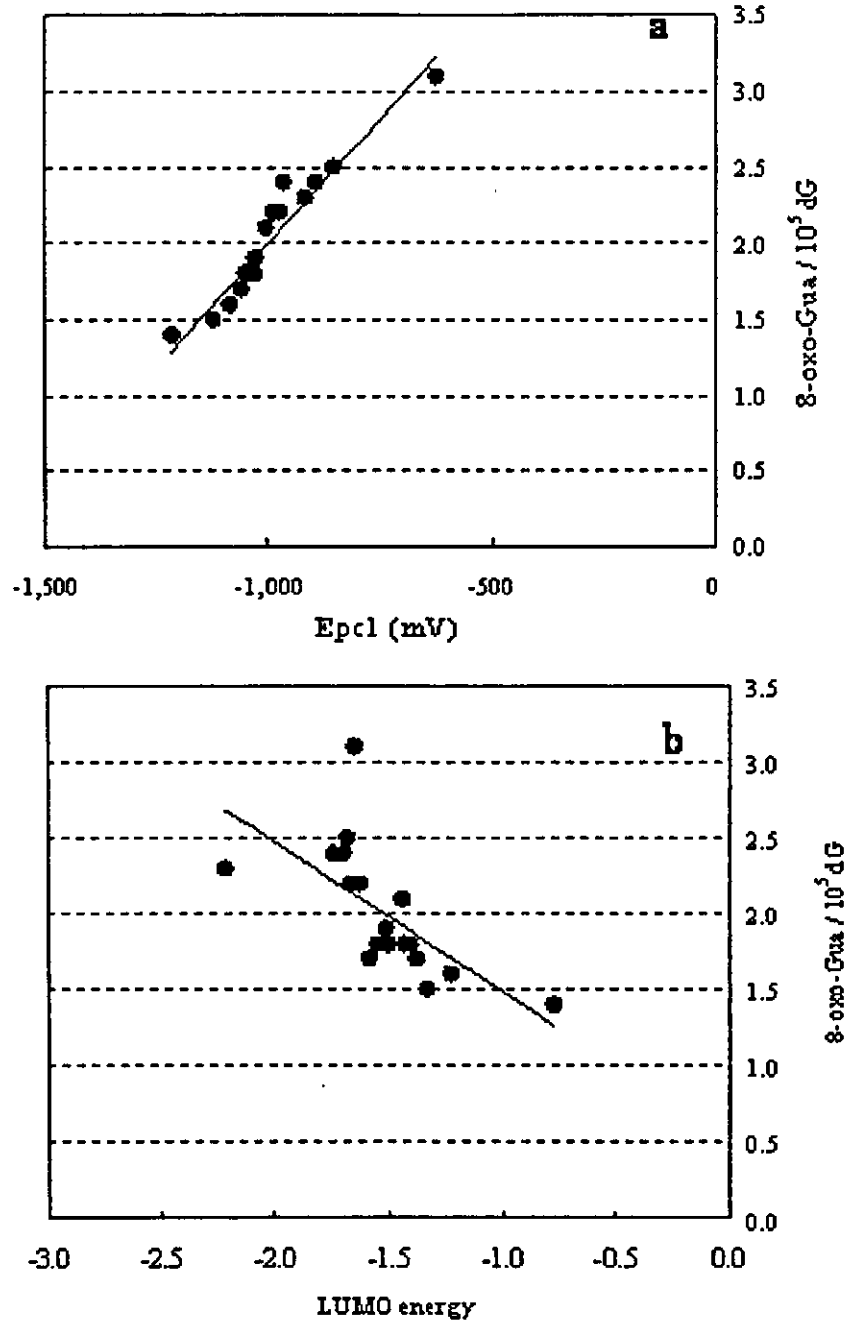

FIGURE 4. Correlation between 8-oxo-Gua formation, and the first reduction potentials (a) and LUMO energy (b) of NAPhs. (a) $r = 0.924$; (b) $r = 0.428$.

positions 2, 3, 6, and 7 were almost coplanar to the phenanthrene rings and were potent mutagens. NPhs substituted on positions 1, 8, 9, and 10 were noncoplanar because of steric hindrance of the aromatic proton at the peri position, with dihedral angles varying from 10° to 65°.

On the other hand, 8-oxo-Gua formed on the guanine residue on DNA is well known as cause of oxidative damage due to environmental

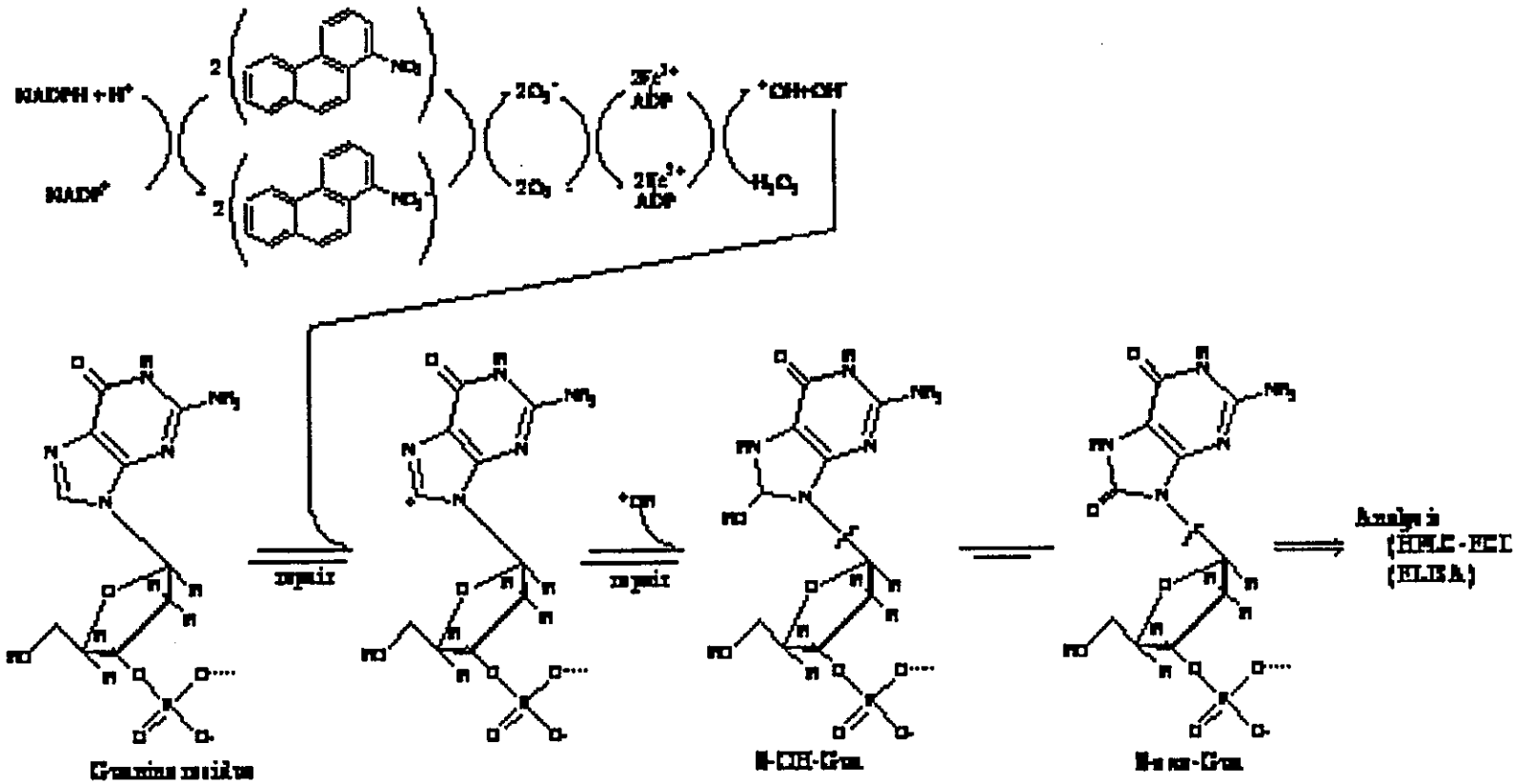

FIGURE 5. Possible mechanisms of oxidative damage in primary rat hepatocytes.

chemicals (18). By using primary rat hepatocytes, 8-oxo-Gua was effectively caused oxidative damage by generation of oxygen and hydroxyl radicals that were induced by nitro groups of NPhs and NAPhs. Thus, 8-oxo-Gua was effectively detected in primary rat hepatocytes by treatment with NPhs and NAPhs, and the induction was closely correlated with their chemical features; primary rat hepatocytes prepared in our laboratory effectively activated these derivatives, suggesting that cytochrome p450 in primary rat hepatocytes has sufficient enzymes to form 8-oxo-Gua. Primary rat hepatocytes showed growth regulation at the beginning of carcinogenesis (19), and in this study, 8-oxo-Gua formation by treatment of 4-NQO, a carcinogen, was observed with dose dependency (Figure 2). Similarly, 8-oxo-Gua formation by treatment with NPhs and NAPhs was significantly correlated with the first reduction potentials, and with LUMO energy for NPhs but not NAPhs. This was due to the fact that nitro groups of NPhs and NAPhs generated OH radicals in the metabolic pathway by microsome enzymes, and radical anions occurred at the 8-position of the guanine residue involving hydroxyl radicals in the presence of heme iron. This suggested that the formation of 8-oxo-Gua was promoted by primary rat hepatocytes. This was roughly the same as the results of many investigators who found increasing 8-oxo-Gua in peripheral lung tissue (17, 20–22).

It was reported that carboxylic acid derivatives of NPhs might induce multiple tumors in aristolochic acid (a herbal drug) patients (23). It was found that induction of mutagens and carcinogens caused the formation of a cyclic nitrenium ion with a decolorized charge by metabolic activation in microsomal enzymes (24–25). NPh derivatives are ubiquitous mutagens in environmental materials, but no NPhs or NAPhs have been detected in plant extracts.

REFERENCES

1. P. P. Fu, M. W. Chou, D. W. Miller, G. L. White, R. H. Heflich, and F. A. Beland, The Orientation of the Nitro Substituent Predicts the Direct-Acting Bacterial Mutagenicity of Nitrated Polycyclic Aromatic Hydrocarbons, *Mutation Res.* 143 (1985):173–181..
2. P. P. Fu, Y.-M. Zhang, R. H. Heflich, Y.-K. Wang, and J.-S. Lai, Effect of the Orientation of Nitro Substituent on the Bacterial Mutagenicity of Dinitrobenzo[*e*]pyrenes, *Mutation Res.* 225 (1989):1211–1225.
3. P. P. Fu, H. Jung, L. S. Von Tungeln, and R. H. Heflich, Mutagenicity of Mononitrodihydrobenzo[*a*]pyrenes, *Mutation Res.* 245 (1990):277–285.
4. H. Jung, A. U. Shaikh, R. H. Heflich, and P. P. Fu, Nitro Group Orientation, Reduction Potential, and Direct-Acting Mutagenicity of Nitro-Polycyclic Aromatic Hydrocarbons, *Environ. Mol. Mutagen.* 17 (1991):169–180.

5. G. Klopman and H. S. Rosenkranz, Structural Requirements for the Mutagenicity of Environmental Nitroarenes, *Mutation Res.* 126 (1984):227–238.
6. H. S. Rosenkranz, C. S. Michell, and G. Klopman, Artificial Intelligence and Bayesian Decision Theory in the Prediction of Chemical Carcinogens, *Mutation Res.* 150 (1985):1–11.
7. W. A. Vance and D. E. Levin, Structural Features of Nitroaromatics that Determine Mutagenic Activity in *Salmonella typhimurium*, *Environ. Mutagen.* 6 (1984):797–811.
8. T. Hirayama, T. Watanabe, M. Akita, S. Shimomura, Y. Fujioka, S. Ozasa, and S. Fukui, Relationships Between Structure of Nitrated Arenes and Their Mutagenicity in *Salmonella typhimurium*; 2- and 2,7-Nitro Substituted Fluorene, Phenanthrene and Pyrene, *Mutation Res.* 209 (1988):67–74.
9. N. Sera, K. Fukuhara, N. Miyata, and H. Tokiwa, Mutagenicity of Nitrophenanthrene Derivatives for *Salmonella typhimurium*: Effects of Nitroreductase and Acetyltransferase, *Mutation Res.* 349 (1996):137–144.
10. H. Tokiwa and Y. Ohnishi, Mutagenicity and Carcinogenicity of Nitroarenes and Their Sources in the Environment, *CRC Crit. Rev. Toxicol.* 17 (1986):23–60.
11. H. Tokiwa, N. Sera, K. Fukuhara, H. Utsumi, S. Sasaki, and N. Miyata, Structural Activity Relationship Between *Salmonella*-Mutagenicity and Nitro-Orientation of Nitroazaphenanthrenes, *Chemico-Biol. Interact.* 146 (2003):19–23.
12. M. Inoue, T. Osaki, M. Noguchi, S. Hirohashi, K. Yasumoto, and H. Kasai, Lung Cancer Patients Have Increased 8-Hydroxydeoxyguanosine Levels in Peripheral Lung Tissue DNA, *Jpn. J. Cancer Res.* 89 (1998):691–695.
13. H. Tokiwa, N. Sera, Y. Nakanishi, and M. Sagai, 8-Hydroxyguanosine formed in Human Lung Tissues and the Association with Diesel Exhaust Particles, *Free Radic. Biol. Med.* 27 (1999):1251–1258.
14. M. Nakajima, T. Takeuchi, and K. Morimoto, Determination of 8-Hydroxydeoxyguanosine in Human Cells under Oxygen-Free Conditions, *Carcinogenesis* 17 (1996):787–791.
15. H. Kasai, N. Iwamoto-Tanaka, T. Miyata, K. Kawanami, S. Kawanami, R. Kido, and M. Ikeda, Lifestyle and Urinary 8-Hydroxydeoxyguanosine, a Marker of Oxidative DNA Damage: Effects of Exercise, Working Conditions, Meat Intake, Body Mass Index, and Smoking, *Jpn. J. Cancer Res.* 92 (2001): 9–15.
16. H. Tokiwa, N. Sera, Y. Nakanishi, and M. Sagai, Formation of 8-Hydroxyguanosine by Purified Lung Particles and Involvement of Alveolar Macrophages, *Chemico-Biol. Interact.* (in press).
17. K. Fukuhara, M. Takei, H. Kageyama, and N. Miyata, Di- and Trinitrophenanthrenes: Synthesis, Separation, and Reduction Property, *Chem. Res. Toxicol.* 8 (1995):47–54.
18. S. Shibutani, M. Takeshita, and A. P. Grollman, Insertion of Specific Bases During DNA Synthesis Past the Oxidation-Damaged Base 8-oxodG, *Nature* 349 (1991): 431–434.
19. A. Low-Baselli, K. Hufnagl, W. Parzefall, P. Schulte-Hermann, and B. Grasl-Kranpp, Initiated Rat Hepatocytes in Primary Culture: A Novel Tool to Study Alterations in Growth Control During The First Stage of Carcinogenesis, *Carcinogenesis* 21 (2000):79–86.

20. M. Lodovici, C. Casalini, R. Cariaggi, L. Michelucci, and P. Dolara, Levels of 8-Hydroxydeoxyguanosine as a Marker of DNA Damage in Human Leukocytes, *Free Radic. Biol. Med.* 28 (2000):13–17.
21. M. Nagashima, H. Kasai, J. Yokota, Y. Nagamachi, T. Ichinose, and M. Sagai, Formation of an Oxidative DNA Damage, 8-Hydroxydeoxyguanosine, in Mouse Lung DNA after Intratracheal Instillation of Diesel Exhaust Particles and Effects of High Dietary Fat and Beta-Carotene on this Process, *Carcinogenesis* 16 (1995):1441–1445.
22. H. Tokiwa, N. Sera, K. Horikawa, Y. Nakanishi, and N. Shigematu, The Presence of Mutagens/carcinogens in the Excised Lung and Analysis of Lung Cancer Induction, *Carcinogenesis* 14 (1993):1933–1938.
23. V. M. Arlt, M. Stiborova, and H. H. Schmeiser, Aristolochic Acid as a Probable Human Cancer Hazard in Herbal Remedies: A Review, *Mutagenesis* 17 (2002):265–277.
24. H. H. Schmeiser, C. A. Bieler, M. Wiessler, C. van Ypersele de Strihou, and J. P. Cosyns, Detection of DNA Adducts Formed by Aristolochic Acid in Renal Tissue from Patients with Chinese Herbs Nephropathy, *Cancer Res.* 56 (1996):2025–2028.
25. H. Schmeiser, E. Frei, M. Wiessler, and M. Stiborova, Comparison of DNA Adduct Formation by Aristolochic Acids in Various in Vitro Activation Systems by 32P-Post-labelling: Evidence for Reductive Activation by Peroxidases, *Carcinogenesis* 18 (1997):1055–1062.

A Planar Catechin Analogue Having a More Negative Oxidation Potential than (+)-Catechin as an Electron Transfer Antioxidant against a Peroxyl Radical

Ikuo Nakanishi,[†,‡] Kei Ohkubo,[†] Kentaro Miyazaki,[§,∥] Wataru Hakamata,[§] Shiro Urano,[∥] Toshihiko Ozawa,[†] Haruhiro Okuda,[§] Shunichi Fukuzumi,*[,†] Nobuo Ikota,*[,‡] and Kiyoshi Fukuhara*[,§]

Redox Regulation Research Group, Research Center for Radiation Safety, National Institute of Radiological Sciences, Inage-ku, Chiba 263-8555, Japan, Department of Material and Life Science, Graduate School of Engineering, Osaka University, CREST, Japan Science and Technology Agency, Suita, Osaka 565-0871, Japan, Division of Organic Chemistry, National Institute of Health Sciences, Setagaya-ku, Tokyo 158 8501, Japan, and Department of Applied Chemistry, Shibaura Institute of Technology, Minato-ku, Tokyo 108-8548, Japan

Received June 30, 2003

The hydrogen transfer reaction of antioxidative polyphenol with reactive oxygen species has proved to be the main mechanism for radical scavenging. The planar catechin ($\mathbf{P1H_2}$), in which the catechol and chroman structure in (+) catechin ($\mathbf{1H_2}$) are constrained to be planar, undergoes efficient hydrogen atom transfer toward galvinoxyol radical, showing an enhanced protective effect against the oxidative DNA damage induced by the Fenton reaction. The present studies were undertaken to further characterize the radical scavenging ability of $\mathbf{P1H_2}$ in the reaction with cumylperoxyl radical, which is a model radical of lipid peroxyl radical for lipid peroxidation. The kinetics of hydrogen transfer from catechins to cumylperoxyl radical has been examined in propionitrile at low temperature with use of ESR, showing that the rate of hydrogen transfer from $\mathbf{P1H_2}$ is significantly faster than that from $\mathbf{1H_2}$. The rate was also accelerated by the presence of $Sc(OSO_2CF_3)_3$. Such an acceleration effect of metal ion indicates that the hydrogen transfer reaction proceeds via metal ion-promoted electron transfer from $\mathbf{P1H_2}$ to oxyl radical followed by proton transfer rather than via a one-step hydrogen atom transfer. The electrochemical case of $\mathbf{P1H_2}$ for the one-electron oxidation investigated by second harmonic alternating current voltammetry strongly supports the two step mechanism for hydrogen transfer, resulting in the enhanced radical scavenging ability.

Introduction

Recently, much attention has been directed to the possibility of natural antioxidants, such as flavonoids, vitamin C, vitamin E, and β-carotene, as chemopreventive agents against oxdative stress and associated diseases (*1*−*3*). The generation of free radicals, such as hydroxyl radical (•OH) and superoxide anion ($O_2^{\bullet-}$), in biological systems is regarded as an important event contributing to the oxidative stress phenomena and one associated with many diseases, e.g., inflammentation, heart disease, cancer, and Alzheimer's (*4*−*6*). Flavonoids are plant phenolic compounds, which are widely distributed in foods and beverages and are extensively studied for their antioxidative and cytoprotective properties in various biological models (*7*−*9*). The antioxidative effects of flavonoids are believed to come from their inhibition of free radical processes in cells at three different levels: an initiation, by scavenging of $O_2^{\bullet}$ (*10*, *11*); lipid peroxidation, by reaction with peroxyl or lipid peroxyl radicals (*12*); and the formation of •OH, probably by chelating iron ions (*13*). Besides their beneficial effects, there is also considerable evidence that flavonoids themselves are mutagenic (*14*, *15*) or carcinogenic (*16*) and show DNA damaging activity (*17*, *18*). Quercetin is a typical flavonoid that has been investigated as a potential chemopreventive agent against certain carcinogens (*19*, *20*). The chemistry of quercetin is predictive of its free radical scavenging ability. However, in biological systems, it was clearly demonstrated that quercetin could behave as both antioxidant and prooxidant. That is, dietary administration of excess quercetin induced renal tubule adenomas and adenocarcinomas in male rats (*21*) and induced intestinal and bladder cancer in rats (*22*). As other polyphenolic compounds, flavonoids may not show the sufficient antioxidative effects into the cells because of their hydrophilic properties, which impede the cell membrane translocation step (*23*). Therefore, much consideration to the safety should be required, when a large quantity of flavonoid is used as medicine for cancer chemoprevention.

In addition to the studies of natural antioxidants used for cancer chemoprevention or nutrition supplements, development of novel antioxidants that show improved radical scavenging activities has attracted considerable interest to remove reactive oxygen species (ROS), such as $O_2^{\bullet-}$ and •OH (*24*). We have previously reported that a planar catechin derivative ($\mathbf{P1H_2}$) (Figure 1), synthesized in the reaction of (+)-catechin ($\mathbf{1H_2}$) with acetone

* To whom correspondence should be addressed. Tel: 81-3 3700 1141. Fax: 81-3 3707 6950. E-mail: fukuhara@nihs.go.jp.
† National Institute of Radiological Sciences.
‡ Osaka University, CREST, Japan Science and Technology Agency.
§ National Institute of Health Sciences.
∥ Shibaura Institute of Technology.

10.1021/tx034134c CCC: $27.50
Published on Web 12/03/2003

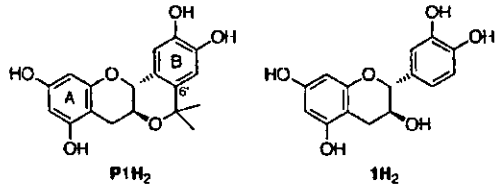

Figure 1. Chemical structures of planar catechin ($P1H_2$) and (+)-catechin ($1H_2$).

in the presence of BF_3·Et_2O (*25, 26*), shows an enhanced protective effect against the oxidative DNA damage induced by the Fenton reaction without the prooxidant effect, which is usually observed in the case of $1H_2$. The spectroscopic and kinetic studies have demonstrated that the rate of hydrogen transfer from $P1H_2$ to galvinoxyl radical (G•), a stable oxygen-centered radical, is about 5-fold faster than that of hydrogen transfer from the native $1H_2$ to G• (*26*). We have also demonstrated that the $O_2^{\bullet-}$ generating ability of the dianion form of $P1H_2$ generated in the reaction of $P1H_2$ with 2 equiv of Bu_4NOMe in deaerated acetonitrile (MeCN) is much lower than that of $1H_2$, suggesting that $P1H_2$ may be a promising novel antioxidant with reduced prooxidant activity (*27*). In addition, as compared with the hydrophilic $1H_2$, the lipophilic property of $P1H_2$, which is very soluble in alcohol, ether, and tetrahydrofuran, seems to give rise to its antioxidative activity into cell membrane.

We report herein that $P1H_2$ can also scavenge cumylperoxyl radical ($PhCMe_2OO^•$) more efficiently than $1H_2$. $PhCMe_2OO^•$, while much less reactive than alkoxyl radicals, is known to follow the same pattern of relative reactivity with a variety of substrates (*28–30*). The effect of a metal ion on the rate of hydrogen transfer from $P1H_2$ to $PhCMe_2OO^•$ was also examined in order to distinguish between the one-step hydrogen atom transfer and the electron transfer mechanisms in the radical scavenging reaction of $P1H_2$ (*31*). The one-electron oxidation potential (E_{ox}^9) of $1H_2$ as well as that of $P1H_2$ in MeCN was determined by the second-harmonic alternating current voltammetry (SHACV). The combination of kinetic and electrochemical results obtained in this study provides confirmative bases to develop novel antioxidants that show improved radical scavenging activities.

Materials and Methods

Materials. A planar catechin derivative ($P1H_2$) was synthesized according to the literature procedure (*26*). (+) Catechin ($1H_2$) was purchased from Sigma. Di *tert* butyl peroxide was obtained from Nacalai Tesque Co., Ltd., and purified by chromatography through alumina, which removes traces of the hydroperoxide. Cumene was purchased from Wako Pure Chemical Industries Ltd., Japan. Tetra *n* butylammonium perchlorate (TBAP) used as a supporting electrolyte was recrystallized from ethanol and dried under vacuum at 313 K. MeCN and propionitrile (EtCN) used as solvent were purified and dried by the standard procedure (*32*).

Spectral and Kinetic Measurements. Kinetic measurements for the hydrogen transfer reactions between catechins and cumylperoxyl radical were performed on a JEOL X band spectrometer (JES ME LX) at 203 K. Typically, photoirradiation of an oxygen saturated EtCN solution containing di *tert* butyl peroxide (1.0 M) and cumene (1.0 M) with a 1000 W high-pressure Mercury lamp resulted in formation of cumylperoxyl radical ($PhCMe_2OO^•$; g = 2.0156), which could be detected at low temperatures. The g values were calibrated by using an Mn^{2+} marker. Upon cutting off the light, the decay of the ESR intensity was recorded with time. The decay rate was accelerated by the presence of $P1H_2$ (1.0×10^{-4} M). Rates of hydrogen transfer from $P1H_2$ to $PhCMe_2OO^•$ were monitored by measuring the decay of the ESR signal of $PhCMe_2OO^•$ in the presence of various concentrations of $P1H_2$ in EtCN at 203 K. Pseudo first-order rate constants were determined by a least squares curve fit using an Apple Macintosh personal computer. The first-order plots of $\ln(I - L)$ vs time (I and L are the ESR intensity at time t and the final intensity, respectively) were linear for three or more half lives with the correlation coefficient, $\rho > 0.99$. In each case, it was confirmed that the rate constants derived from at least five independent measurements agreed within an experimental error of ±5%.

Scheme 1

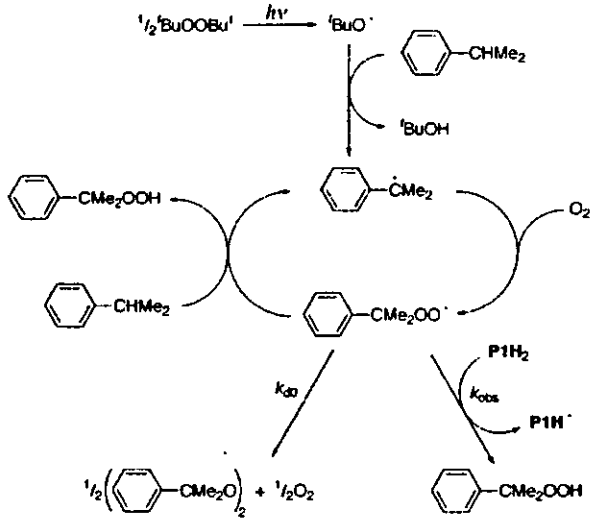

Electrochemical Measurements. The SHACV (*33–38*) measurements of $1H_2$ and $P1H_2$ were performed on an ALS 630A electrochemical analyzer in deaerated MeCN containing 0.10 M TBAP as a supporting electrolyte at 298 K. The platinum working electrode was polished with BAS polishing alumina suspension and rinsed with acetone before use. The counter electrode was platinum wire. The measured potentials were recorded with respect to an $Ag/AgNO_3$ (0.01 M) reference electrode. The one-electron oxidation potentials (E_{ox}^9) (vs $Ag/AgNO_3$) were converted into those vs SCE by addition of 0.29 V (*39*).

Results

Hydrogen Transfer from Catechins to Cumylperoxyl Radical. Direct measurements of the rates of hydrogen transfer from a planar catechin derivative ($P1H_2$) to cumylperoxyl radical were performed in EtCN at 203 K by means of ESR. The photoirradiation of an oxygen-saturated EtCN solution containing di *tert* butylperoxide (Bu^tOOBu^t) and cumene with a 1000 W high-pressure mercury lamp results in formation of cumylperoxyl radical ($PhCMe_2OO^•$), which was readily detected by ESR. The cumylperoxyl radical is formed via a radical chain process shown in Scheme 1 (*40–44*).

The photoirradiation of Bu^tOOBu^t results in the homolytic cleavage of the O–O bond to produce $Bu^tO^•$ (*45–51*), which abstracts a hydrogen from cumene to give cumyl radical, followed by the facile addition of oxygen to cumyl radical. The cumylperoxyl radical can also abstract a hydrogen atom from cumene in the propagation step to yield cumene hydroperoxide, accompanied by regeneration of cumyl radical (Scheme 1) (*52, 53*). In the termination step, cumylperoxyl radicals decay by a bimolecular reaction to yield the corresponding peroxide

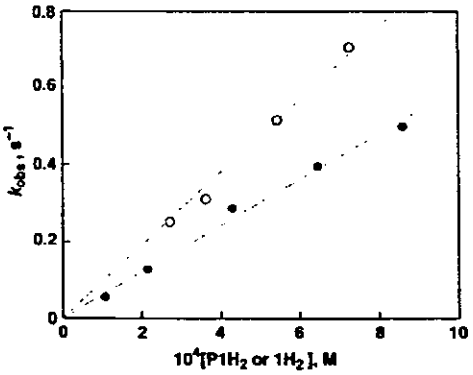

Figure 2. Plots of k_{obs} vs **P1H$_2$** (white circles) and vs **1H$_2$** (black circles) for the reactions of catechins (**P1H$_2$** and **1H$_2$**) with cumylperoxyl radical in EtCN at 203 K.

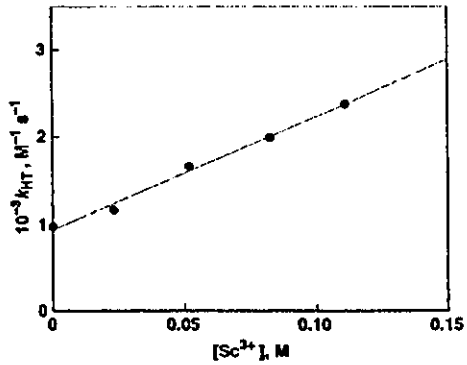

Figure 3. Plot of k_{HT} vs [Sc^{3+}] in the reaction of **P1H$_2$** to cumylperoxyl radical in the presence of $Sc(OSO_2CF_3)_3$ in EtCN at 203 K.

and oxygen (Scheme 1) (*41*, *42*). When the light is cut off, the ESR signal intensity decays obeying second-order kinetics due to the bimolecular reaction in Scheme 1.

In the presence of **P1H$_2$**, however, the decay rate of cumylperoxyl radical after cutting off the light becomes much faster than that in the absence of **P1H$_2$**. The decay rate in the presence of **P1H$_2$** (1.0×10^{-4} M) obeys pseudo first-order kinetics. This decay process is ascribed to hydrogen transfer from **P1H$_2$** to cumylperoxyl radical (Scheme 1). The pseudo-first-order rate constants increase with increasing **P1H$_2$** concentration ([**P1H$_2$**]) to exhibit first-order dependence on [**P1H$_2$**] as shown in Figure 2. From the slope of the linear plot of k_{obs} vs concentration of **P1H$_2$** is determined the second-order rate constant (k_{HT}) for the hydrogen transfer from **P1H$_2$** to cumylperoxyl radical as 9.7×10^2 M^{-1} s^{-1} in EtCN at 203 K.

Figure 2 also shows the linear plot of k_{obs} vs the concentration of (+) catechin (**1H$_2$**) for the reaction of **1H$_2$** with cumylperoxyl radical in EtCN at 203 K. The k_{HT} value for **1H$_2$** was also determined in the same manner as 6.0×10^2 M^{-1} s^{-1} (*31*). Thus, as in the case of galvinoxyl radical (*26*), the hydrogen transfer rate from **P1H$_2$** to cumylperoxyl radical is significantly faster than that from **1H$_2$**.

We have recently reported that the hydrogen transfer from **1H$_2$** to galvinoxyl or cumylperoxyl radical proceeds via electron transfer from **1H$_2$** to galvinoxyl or cumylperoxyl radical, which is accelerated by the presence of metal ions, such as Mg^{2+} and Sc^{3+}, followed by proton transfer (*31*). In such a case, the coordination of the metal ion to the one-electron reduced species of galvinoxyl or cumylperoxyl radical may stabilize the product, resulting in acceleration of the electron transfer process. In this context, the effect of a metal ion on the k_{HT} value of **P1H$_2$** was examined. As in the case of **1H$_2$**, the hydrogen transfer from **P1H$_2$** to cumylperoxyl radical was significantly accelerated by the presence of $Sc(OSO_2CF_3)_3$ as shown in Figure 3. Thus, the hydrogen transfer from **P1H$_2$** to cumylperoxyl radical also proceeded via electron transfer from **P1H$_2$** to cumylperoxyl radical followed by proton transfer from **P1H$_2$**$^{\bullet+}$ to one-electron reduced species cumylperoxyl radical as shown in Scheme 2.

The larger k_{HT} value of **P1H$_2$** as compared to that of **1H$_2$** may be ascribed to the stability of the radical cation of **P1H$_2$** (**P1H$_2$**$^{\bullet+}$), which is produced in the electron transfer from **P1H$_2$** to cumylperoxyl radical. The electron donating *i*propyl group at the B ring of **P1H$_2$** may

Scheme 2

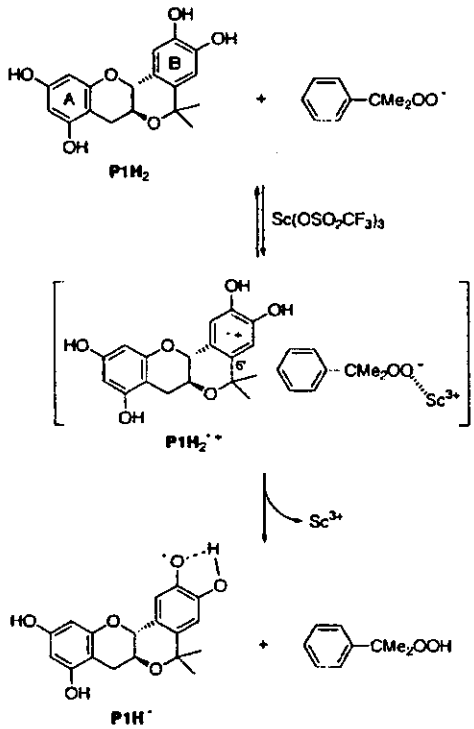

significantly stabilize **P1H$_2$**$^{\bullet+}$, resulting in the acceleration of the electron transfer step. In such a case, the one-electron oxidation potential of **P1H$_2$** is expected to be more negative than that of **1H$_2$**.

One-Electron Oxidation Potential of a Planar Catechin Analogue. To determine the one-electron oxidation potential of **P1H$_2$**, the cyclic voltammogram of **P1H$_2$** was recorded in MeCN containing 0.1 M TBAP as a supporting electrolyte at 298 K. Two irreversible oxidation (anodic) peaks were observed at 1.22 and 1.41 V vs SCE (data not shown). A similar cyclic voltammogram was obtained for **1H$_2$**, which exhibits irreversible oxidation peaks at 1.16 and 1.35 V vs SCE. This indicates that radical cations of **P1H$_2$** and **1H$_2$** are too unstable at the time scale of CV measurements. The SHACV method is known to provide a superior approach to directly evaluating one-electron redox potential in the presence of the follow up chemical reaction relative to the better known dc and fundamental harmonic ac method (*34*). The

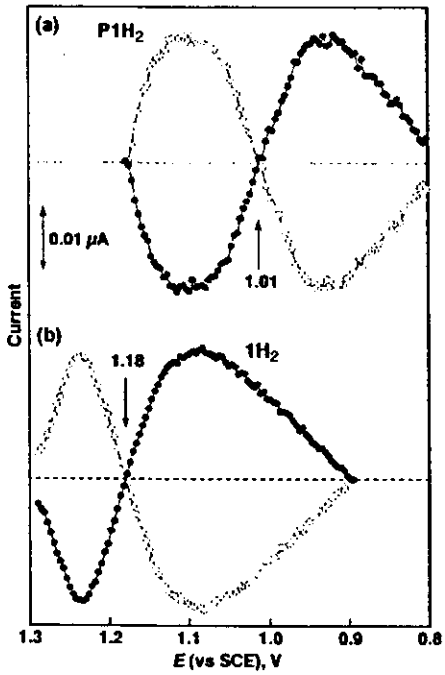

Figure 4. SHACVs of (a) $\mathbf{P1H_2}$ and (b) $\mathbf{1H_2}$ in deaerated MeCN containing 0.1 M TBAP at 298 K. Scan rate, 4 mV s^{-1}; working electrode, Pt.

SHACV method was applied to determine the one-electron oxidation potentials (E_{ox}^0) of $\mathbf{P1H_2}$ and $\mathbf{1H_2}$ in deaerated MeCN containing 0.1 M TBAP at 298 K. Figure 4 shows the SHACV of $\mathbf{P1H_2}$ and $\mathbf{1H_2}$. The E_{ox}^0 value of $\mathbf{P1H_2}$ thus determined (1.01 V vs SCE) is significantly more negative than that of $\mathbf{1H_2}$ (1.18 V vs SCE) as expected above. Thus, $\mathbf{P1H_2}$ may undergo one-electron oxidation by cumylperoxyl radical more easily than $\mathbf{1H_2}$, showing excellent radical scavenging abilities.

Discussion

The primary goal of this project is to develop a novel antioxidant, which can be positively utilized for clinical treatment and/or chemoprevention of diseases associated with ROS. There are two kinds of strategy in considering the development of synthetic antioxidants: one is a design of a new type of antioxidant, the structure of which is different from the natural antioxidant, and the other is a modification of natural antioxidants to improve its antioxidative capacities. A recent topic on the synthetic antioxidants is a development and clinical application of edaravone (3-methyl-1-phenyl-2-pyrazolin-5-one, MCI-186). Edaravone has been reported to show potent free radical scavenging actions toward ROS, such as $O_2^{\bullet-}$, H_2O_2, and HClO, which may be involved in the tissue destructive effects of reperfusion after ischemia (*54*–*56*). As a neuroprotective agent, edaravone has been clinically prescribed in Japan since 2001 to treat patients with cerebral ischemia. Regarding flavonoids, there are many reports for the synthetic derivatives to exert prominent chemopreventive effects toward oxidative stress derived injury. However, only a few studies on the synthetic flavonoids, which were aimed at the improved radical scavenging ability, have been reported. Flavopiridol is a chlorinated derivative of flavone, which is currently in clinical development for the treatment of advanced cancer, including ovarian cancer (*57*, *58*). Flavopiridol is an inhibitor of cycline-dependent kinases to modulate cell cycle (*59*), and radical scavenging mechanism is not involved in the expression of anticancer effects of this compound.

The planar catechin ($\mathbf{P1H_2}$), which has been detected in mere trace amounts in nature (*60*), is easily synthesized by the reaction of $\mathbf{1H_2}$ and acetone (*26*). The ability of $\mathbf{P1H_2}$ to scavenge oxygen-centered radical, such as galvinoxyl radical, is excellent as compared to that of (+)-catechin and its complete inhibition of oxidative DNA damage induced by metal-catalyzed generation of hydroxyl radical (*26*), as well. Therefore, $\mathbf{P1H_2}$ may exert its antioxidative capacities by scavenging reactive oxygen radicals in many types of biologically generating systems. The present study was focused on the reaction of $\mathbf{P1H_2}$ to cumylperoxyl radical, a model radical of lipid peroxyl radical formed in a radical chain reaction of lipid peroxidation. The processes of lipid peroxidation concomitant with the formation of lipid peroxyl radicals are detrimental to the viability of the cell. The biophysical consequences of peroxidation on membrane phospholipids can be both extensive and highly destructive, provoking diseased states such as atherosclerosis, heart attacks, cancer, ischaemia/repulsion injury, and even the aging process as a whole (*61*). The ability of antioxidant to scavenge peroxyl radicals and block lipid peroxidation raises the possibility that it may protect against the many types of free radical associated diseases. As compared with $\mathbf{1H_2}$, $\mathbf{P1H_2}$ showed strong radical scavenging ability toward cumylperoxyl radical formed via a radical chain process, as well as the predominant radical scavenging reaction of $\mathbf{P1H_2}$ to galvinoxyl radical. Lipid peroxyl radical formed by the reaction between a lipid radical and a molecular oxygen is essential for autoxidation of lipid. The peroxyl radical abstracts an allylic hydrogen atom from an adjacent polyunsaturated fatty acid, resulting in a lipid hydroperoxide and a second lipid radical. Therefore, $\mathbf{P1H_2}$ may act as an effective terminator by means of scavenging free radicals in autoxidation of lipids.

Considering the antioxidative mechanism to scavenge peroxyl radical, there are two possibilities in the mechanism of hydrogen transfer reactions, i.e., a one step hydrogen atom transfer or electron transfer followed by proton transfer. The hydrogen transfer reaction from $\mathbf{P1H_2}$ to cumylperoxyl radical accelerated in the presence of the metal ion, indicating that the hydrogen transfer reaction proceeded by the two-step reaction, that is, electron transfer from $\mathbf{P1H_2}$ to cumylperoxyl radical followed by proton transfer from $\mathbf{P1H_2}^{\bullet+}$. Vitamin E is a typical antioxidant to terminate lipid peroxidation, and the hydrogen transfer reaction proceeds via a one step hydrogen atom transfer process, which is due to no effect of metal ion on the hydrogen transfer rate from vitamin E analogue to galvinoxyl radical (*62*). On the other hand, in the case of $\mathbf{1H_2}$, the hydrogen transfer reaction proceeds via electron transfer from $\mathbf{1H_2}$ to oxyl radical followed by proton transfer rather than via a one-step hydrogen atom transfer (*31*), as the case of present results of the $\mathbf{P1H_2}$. The one-electron oxidation potential investigated by the SHACV indicated that the electrochemical oxidation of $\mathbf{P1H_2}$ was easier to progress in comparison with $\mathbf{1H_2}$. The electron transfer mechanism for the radical scavenging reaction of $\mathbf{P1H_2}$ is probably a consequence of its electrochemical ease for one electron oxidation. Judging from the one-electron oxidation po